Supplementary Information

Light-driven Ultrafast Dual C–C Cleavage and Coupling of Dihydroxyacetone into High-purity Carbon monoxide and Ethylene glycol

Fanhao Kong, Hongru Zhou, Zhiwei Chen, Zhaolin Dou, Min Wang*

State Key Laboratory of Fine Chemicals, School of Chemistry, Dalian University of Technology, Dalian, 116024 Liaoning, P. R. China

*E-mail: wangmin@dlut.edu.cn

Table of Contents

Experimental procedures

Reagents

All chemicals used were of analytical grade and used directly without further treatment. 1,3-dihydroxyacetone, hydroxyacetone, 1,3-dichloroacetone, 1,3-dibromoacetone, formic acid, glycolaldehyde dimer, diethylamine, $Pd(PPh_3)_4$, 1-hexyne, DBU, S-butyl thiobenzoate, 4-methoxybenzophenone, chalcone, and deuterium water were purchased from Shanghai Macklin Biochemical Co., Ltd. Acetonitrile, ethanol, methanol, acetic acid, tetrahydrofuran were purchased from Tianjin Kermel Chemical Reagent Co., Ltd. Acetone, cyclohexanone, glucose, fructose, styrene, and dioxane were purchased from Sinopharm Chemical Reagent Co., Ltd. Formaldehyde, glyoxal, and potassium carbonate were purchased from Tianjin Damao Chemical Reagent Factory. Glycolic acid, TEMPO, 3-iodotoluen iodobenzene, 4-iodoanisole, phenylboronic acid, triphenylphosphine, n-butylamine, 1-butanethiol, N,N-diethyl-3-methylbenzamide, CataCXium® A, Cy_2Nme, ethyl p-anisate were purchased from Aladdin Chemistry Co., Ltd. Triethylamine was purchased from XiLong Scientific Co., Ltd. Palladium(II) chloride, $Pd(t\text{-}Bu_3P)_2$, $[Pd(cinnamyl)Cl]_2$, acetone-D6, and methanol-D4 were purchased from Shanghai Energy Chemical Chemical Reagent Co., Ltd. Deionized water was purified by using a Millipore Milli-Q Advantage A10 system. He (>99.999%), Ar (>99.999%), H_2 (>99.999%), CO (>99.999%), CO_2 (>99.999%) were provided by Dalian Junfeng Gas Chemicals Co., Ltd.

Lamp sources

The data involved in this work used three types of ultraviolet lamps.

In the condition optimization section, eight of UVC 3535 LED lamps in series was used and purchased from Shenzhen Taiyi Photoelectric Co., Ltd. Each UVC 3535 LED lamp bead welded to aluminum substrate (1 cm × 1 cm), and its electric power is 2 W with optical power of 40-50 mW, the emission angle is 60°, and the wave length of 275 nm. Commercial handheld 5 W 275 nm LED was used and purchased from ZiGu lighting electrical appliance factory.

In the flow synthesis section, a tubular E27 UVC lamp was used and purchased from Tianchang Kangda UV disinfection lamps factory. Its electric power is 36 W with the wave length of 254 nm.

In the CO generator section, an non-polar submersible UVC lamp was used and purchased from Ningguo Hubang Electronic Technology Co., Ltd. Its electric power is 60 W with the wave length of 254 nm.

Quartz tubes

Sealable straight quartz tubes were made-to-order and purchased from Donghai Jing-Ao quartz products Co., Ltd. The outside diameter is about 1 cm and the length is about 10 cm. The total volume of the internal cavity is approximately 6.5 mL.

Spiral quartz tubes were made-to-order and purchased from Donghai Jing-Ao quartz products Co., Ltd. The diameter for each circle of spiral quartz tubes surrounding the tubular E27 UVC lamp is 49 mm, total circle is 42, and total length is about 6.5 m. The inner diameter and outer diameter of spiral quartz tubes are 1 mm and 3 mm, respectively.

Characterizations

The UV-vis diffuse reflectance spectra were recorded on a Avasoft-2048L fiber optic spectrometer in the range of 200-2500 nm at room temperature. The online mass spectrometer used an online mass spectrometer 200 (BSD-Mass; Beishide Instrument-S&T. Co., Ltd) with Ar flow. The gas chromatography-mass spectrometry (GC-MS) used an Agilent 7890A/5975C instrument equipped with an HP-5 MS column (30 m in length, 0.25 mm in diameter).

Photochemical experiments

Condition optimization experiments were performed by illuminating 0.1 M DHA under 800 rpm stirring for 1 h at room temperature in a sealable straight quartz reaction tube with the changing factors of radiation wavelength, solvent, and atmosphere. Normal conditions are that 0.1 M DHA, 1 mL of H_2O, home-made 16 W 275 nm lamp set by circular arrangement eight of 2 W LED lights in series, irradiation for 1 h, Ar atmosphere, room temperature, stir 800 rpm.

Time-dependent profiles for DHA were collected under normal conditions.

Visualization photolysis for DHA was carried out by one side illuminating 0.1 M DHA solution in a four-way quartz cuvette using a commercial handheld 5 W 275 nm LED.

In situ gas composition detection was performed by one side illuminating 1.0 M DHA solution with stirring of 800 rpm in a sealable quartz reaction tube using a commercial handheld 5 W 275 nm LED. Argon was used carrier gas which transports in situ gas products to online mass spectrometer.

Ex situ gas composition detection was performed by injecting collected gas after reaction to online mass

spectrometer.

Triplet state DHA quenching experiments were performed by illuminating 0.1 M DHA solution for 2 min with adding 0.5 M sodium bromide or sodium iodide.

Radical trapping experiments were performed by illuminating 0.1 M DHA in MeCN and water mixed solvent (9 : 1) for 5 min or 2 h with adding a certain amount TEMPO or styrene, respectively.

Other controlled experiments of various substrates or deuterated solvent were performed under normal conditions.

Photochemical flow experiments were performed using home-built photochemical flow device. The performance parameters for DHA conversion and CO/EG generation were studied with changing the concentration of DHA solution pumped at a fixed flow rate of 0.2 mL min^{-1}.

Gas analysis

The gas products were quantified via the internal standard method by a Tianmei gas chromatograph in Tianmei GC. Tianmei GC equipped with a TCD detector and TDX-01 column (3 m × 2 mm). He was used as the internal standard. The GC peak area was used for calculation. The differential response was calibrated using the response factor. The detailed calculation was as follows:

$$V(CO) = \frac{A(CO)}{A(He)} \times V(He) \times K(CO)$$

$$V(H_2) = \frac{A(H_2)}{A(He)} \times V(He) \times K(H_2)$$

V_{CO}: the volume of produced CO; V_{H_2} : the volume of produced H_2; V_{He}: the He volume injected in the reactor; A_{CO}: the peak area of CO in GC; A_{H_2}: the peak area of H_2 in GC; A_{He}: the peak area of He in GC; K_{CO}: the CO response factor related to He in Tianmei GC; K_{H_2}: the H_2 response factor related to He.

HPLC analysis

High-performance liquid chromatography (HPLC, Shimadzu Prominence LC-20AD) equipped with an ultraviolet-visible detector (UV) and differential refractive index detector (RID) was used to analyze the concentration of substrates and products in the liquid phase. Chromatographic column used a ROA-Organic Acid H^+ column (8 %, 300 × 7.8 mm), the mobile phase was H_2SO_4 (0.05 wt%) solution with the flow rate of 0.5 mL min^{-1}, the column tempoture was 313.15 K, and the UV wavelength was set to 210 nm. And 10 μL of

diluent was injected by an autosampler. The molar amount of liquid phase products were quantified by standard curves.

Calculations

All the calculations have been carried out using Gaussian 16 software package[1]. Geometry optimization have been carried out using Hatree Fock (HF) method, second-order Møller-Plesset perturbation theory (MP2), density functional theory (DFT)[2-4]. The B3LYP functional and the diffuse and polarization functions augmented split valence 6-31++G(d,p) basis set is used for description of molecular orbitals for geometry optimization[5,6]. The time dependent (TD) DFT calculations were performed to calculate the excited state of each species.

Carbonylation reactions by CO generator

Six types of carbonylation reactions were performed based on modified literatures[7-12].

Aminoxarbonylation: the reaction solution of aminoxarbonylation is first obtained in a tube by mixing 3-iodotoluene (0.025 mmol), diethylamine (0.05 mmol), triethylamine (0.05 mmol) and $Pd(PPh_3)_4$ (10 mg) in 1,4-dioxane (0.5 mL). Then, the mixed reaction solution is flash frozen by immersion of reaction tube in liquid nitrogen flash and the reaction tube was evacuated to an internal pressure. Six milliliters of CO produced by CO generator was tranfered and injected in above reaction. The reaction was stirred at 65 °C for 22 h in the oil bath. The product was detected and quantified by mass spectrometry.

Thiocarbonylation: the reaction solution of thiocarbonylation is first obtained in a tube by mixing iodobenzene (0.025 mmol), 1-butanethiol (0.05 mmol), triethylamine (0.05 mmol) and $Pd(PPh_3)_4$ (10 mg) in 1,4-dioxane (0.5 mL). Then, the mixed reaction solution is flash frozen by immersion of reaction tube in liquid nitrogen flash and the reaction tube was evacuated to an internal pressure. Six milliliters of CO produced by CO generator was tranfered and injected in above reaction. The reaction was stirred at 85 °C for 22 h in the oil bath. The product was detected and quantified by mass spectrometry.

Alkoxycarbonylation: the reaction solution of alkoxycarbonylation is first obtained in a tube by mixing 4-iodoanisole (0.025 mmol), triethylamine (0.05 mmol) and $Pd(PPh_3)_4$ (10 mg) in ethanol (0.5 mL). Then, the mixed reaction solution is flash frozen by immersion of reaction tube in liquid nitrogen flash and the reaction tube was evacuated to an internal pressure. Six milliliters of CO produced by CO generator was tranfered and injected in above reaction. The reaction was stirred at 80 °C for 22 h in the oil bath. The product was detected

and quantified by mass spectrometry.

Carbonylative Suzuki coupling: the reaction solution of carbonylative suzuki coupling is first obtained in a tube by mixing 4-iodoanisole (0.025 mmol), phenylboronic acid (0.075 mmol), K_2CO_3 (0.075 mmol) and Palladium(II) chloride (2 mg) in 1,4-dioxane (0.5 mL). Then, the mixed reaction solution is flash frozen by immersion of reaction tube in liquid nitrogen flash and the reaction tube was evacuated to an internal pressure. Six milliliters of CO produced by CO generator was tranfered and injected in above reaction. The reaction was stirred at 80 °C for 24 h in the oil bath. The product was detected and quantified by mass spectrometry.

Double Carbonylation: the reaction solution of double carbonylation coupling is first obtained in a tube by mixing 4-iodoanisole (0.025 mmol), n-butylamine (0.05 mmol), DBU (0.05 mmol) and $Pd(t\text{-}Bu_3P)_2$ (10 mg) in THF solution (0.5 mL). Then, the mixed reaction solution is flash frozen by immersion of reaction tube in liquid nitrogen flash and the reaction tube was evacuated to an internal pressure. Six milliliters of CO produced by CO generator was tranfered and injected in above reaction. The reaction was stirred at 25 °C for 22 h in the oil bath. The reaction product was detected and quantified by mass spectrometry.

Carbonylative Sonogashira: the reaction solution of carbonylative sonogashira coupling is first obtained in a tube by mixing 4-iodoanisole (0.25 mmol), PPh_3 (10 mg), Palladium(II) chloride (3 mg), Et_3N (0.105 mL), H_2O (0.31 mL) and 1-hexyne (0.3 mmol). Then, the mixed reaction solution is flash frozen by immersion of reaction tube in liquid nitrogen flash and the reaction tube was evacuated to an internal pressure. Twenty milliliters of CO produced by CO generator was tranfered and injected in above reaction. The reaction was stirred at 95 °C for 20 h in the oil bath. The product was detected and quantified by mass spectrometry.

Supplementary figures

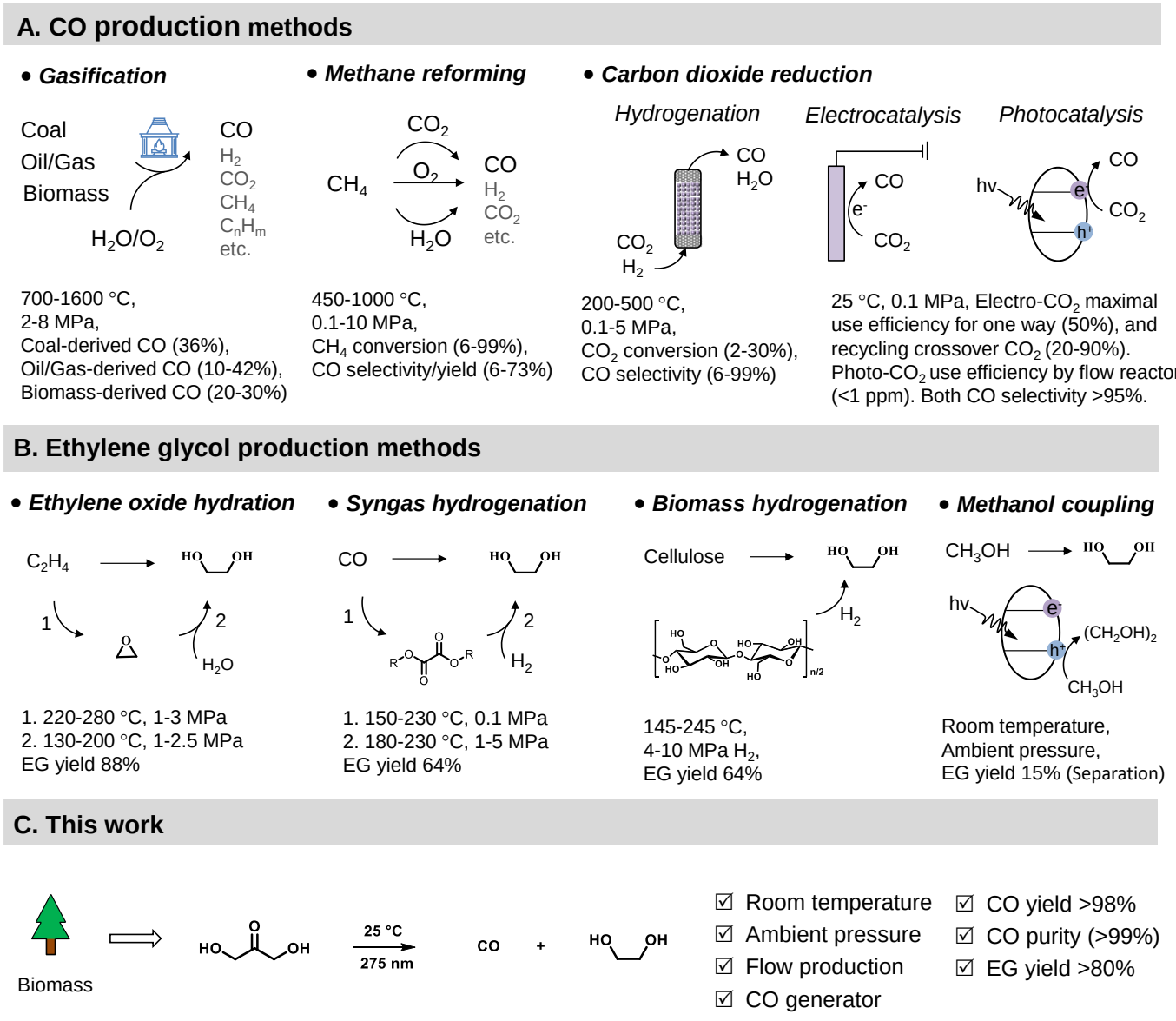

Fig. S1. Method summary for CO and ethylene glycol production. (A) CO production methods including gasification[13-19], methane reforming[20-25], CO_2 hydrogenation[26-29], electrochemical and photocatalytic CO_2 reduction[30,31]. (B) Ethylene glycol production methods including ethylene oxide hydration[32-34], syngas hydrogenation[35], biomass hydrogenation[36-38], and methanol coupling[39,40]. (C) CO production together with ethylene glycol from photolysis of biomass-based dihydroxyacetone.

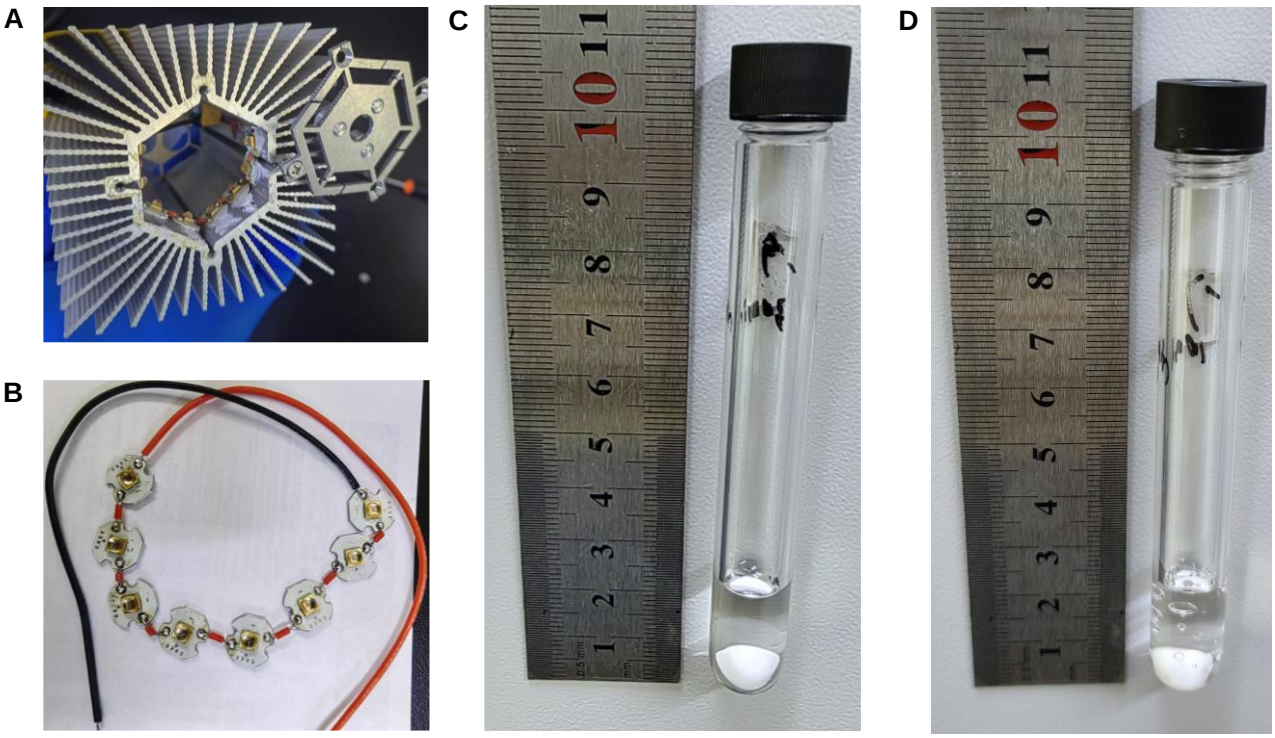

Fig. S2. The home-made lamp set and photoreaction tube for condition optimization of the photolysis of DHA. (A) the home-made lamp set surrounding the heat sink. (B) Eight of 2 W 275 nm LED lights in series. (C) The 1 mL of 0.1 M DHA aqueous solution in photoreaction tube before photolysis. (D) The 1 mL of 0.1 M DHA aqueous solution in photoreaction tube after photolysis for 10 min.

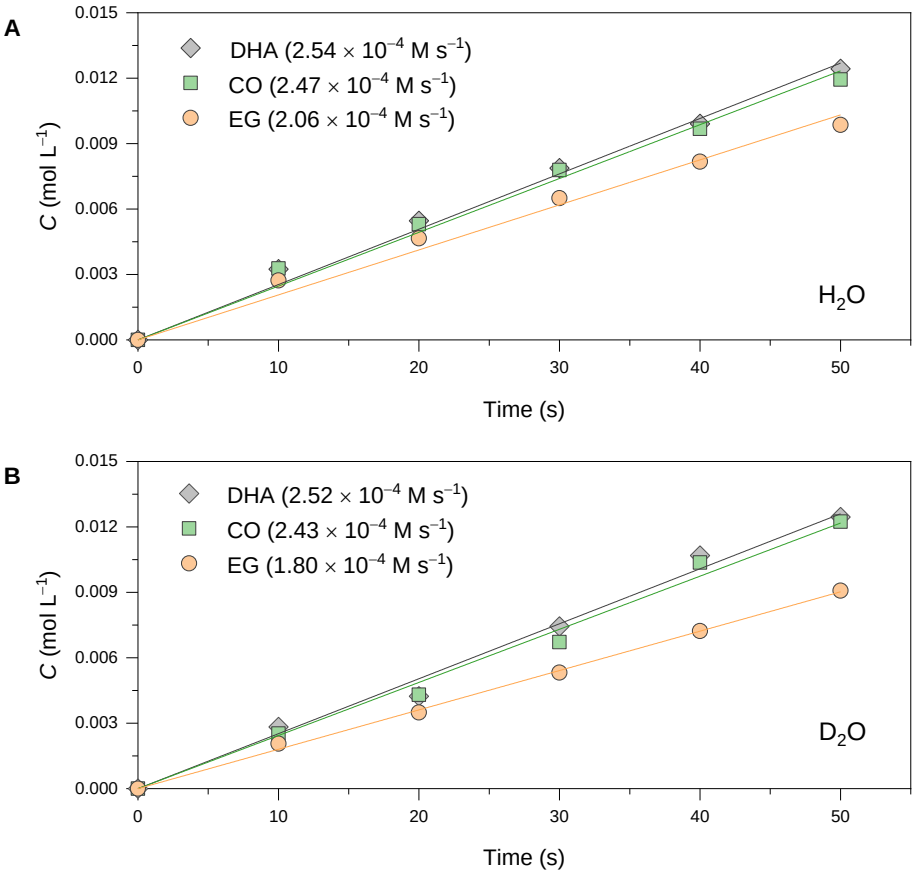

Fig. S3. The reaction kinetics for the photolysis of DHA in (A) H_2O and (B) D_2O solution.

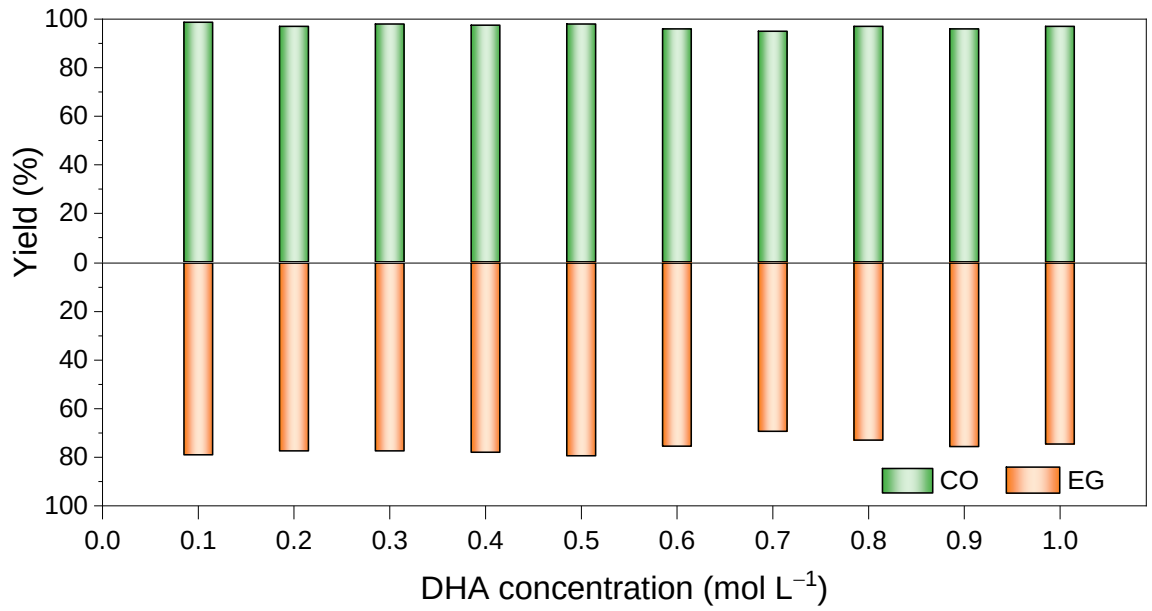

Fig. S4. Photolysis of dihydroxyacetone with different concentrations. Reaction conditions: 0.1-1.0 M DHA, 1 mL of H_2O, home-made 16 W 275 nm lamp set by circular arrangement eight of 2 W LED lights in series, irradiation for 1-5 h, Ar atmosphere, room temperature, stir 800 rpm.

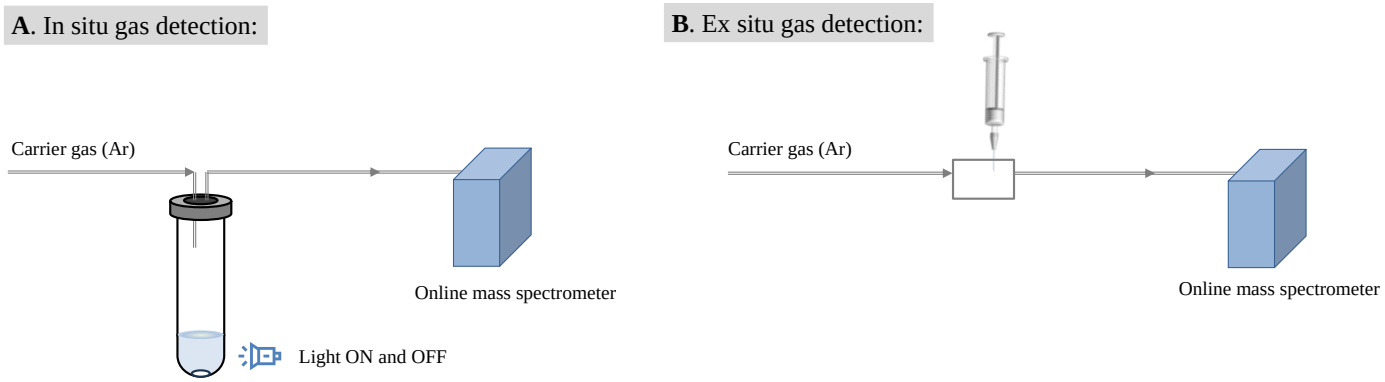

Fig. S5. Gas detection using online mass spectrometer. (A) In situ detection of produced gas by controling light switch. (B) Ex situ detection of produced gas by injection.

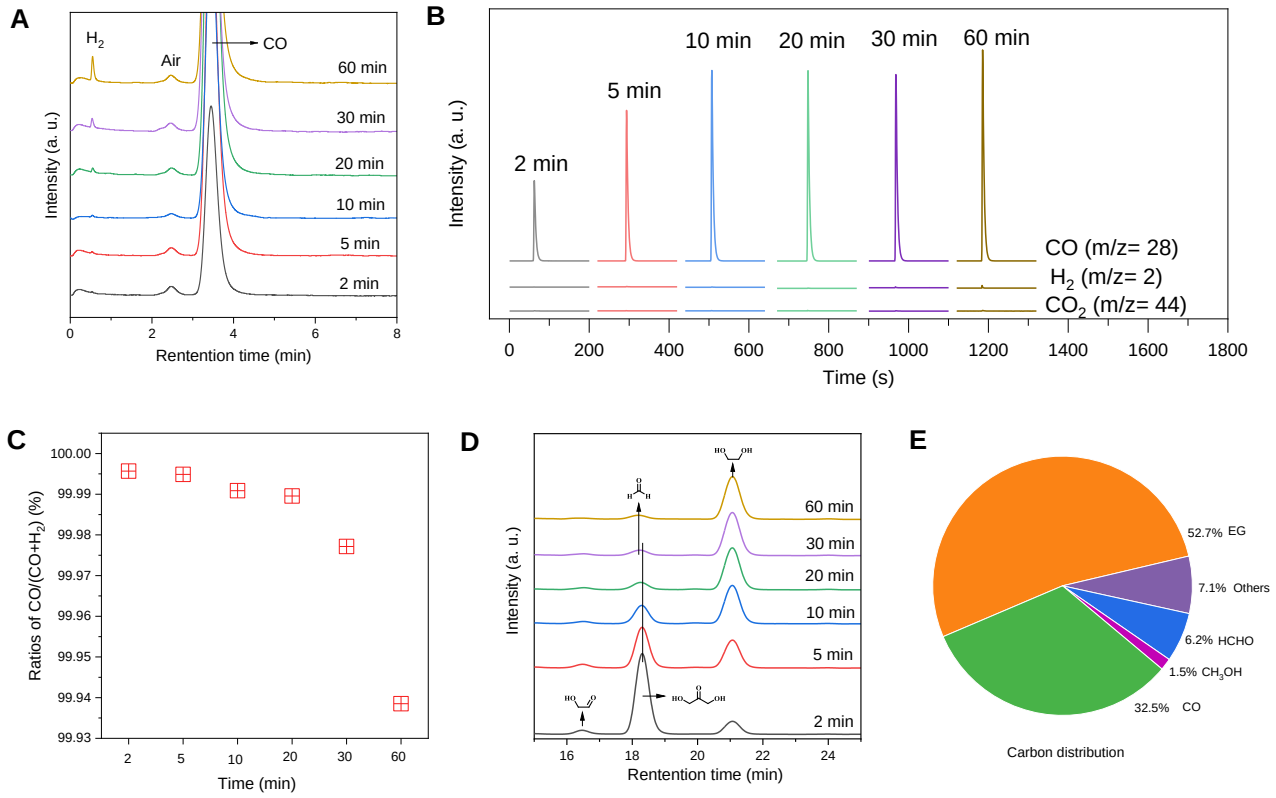

Fig. S6. Time-dependent datum for the photolysis of DHA. (A) Gas chromatograms. (B) Online mass spectrometer chromatograms obtained by ex situ injection detection. (C) The proportion of CO in the obtained gas of CO and H_2. (D) The high-performance liquid chromatograms. (E) Carbon distribution after 1 h. Reaction conditions: 0.1 M DHA, 1 mL of H_2O, home-made 16 W 275 nm lamp set, irradiation for 2-60 min, Ar atmosphere, room temperature, stir 800 rpm.

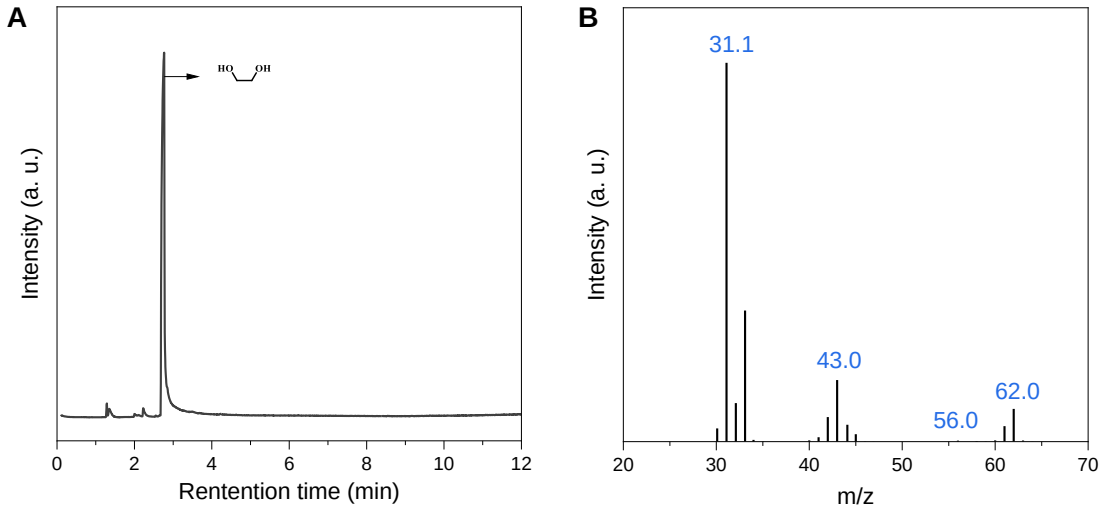

Fig. S7. GC-MS pattern for the photolysis of DHA. (A) GC-MS pattern for the photolysis of DHA. (B) MS spectra in GC-MS pattern at a retention time of 2.8 min. Reaction conditions: 0.1 M DHA, 1 mL of H2O, home-made 16 W 275 nm lamp set by circular arrangement eight of 2 W LED lights in series, irradiation for 1 h, Ar atmosphere, room temperature, stir 800 rpm.

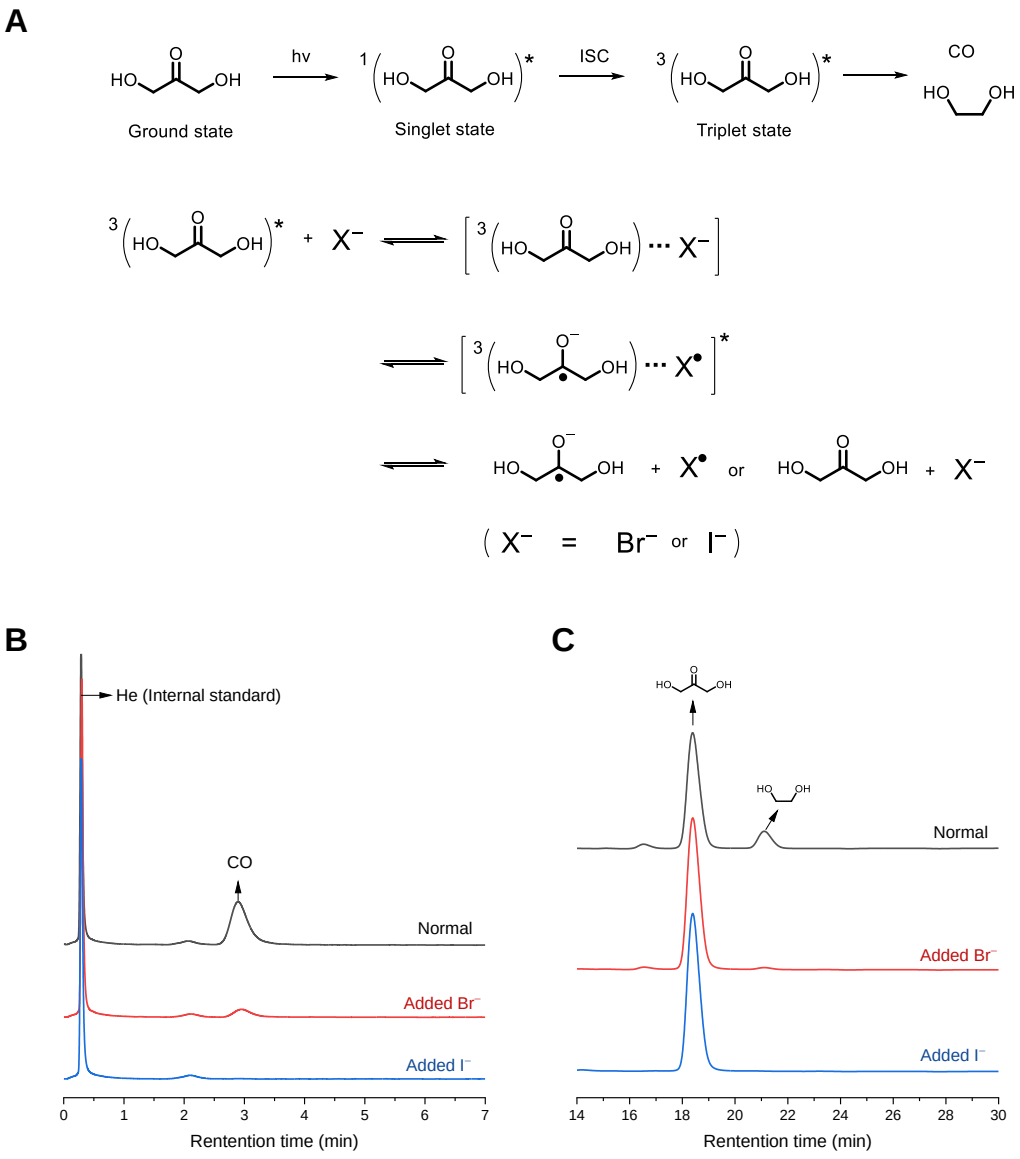

Fig. S8. Triplet state DHA quenching experiments by adding bromide or iodide ions. (A) Triplet state DHA quenching mechanisms. (B) Gas chromatograms. (C) The high-performance liquid chromatograms. Reaction conditions: 0.1 M DHA, 0.5 M NaBr (or NaI), 1 mL of H_2O, home-made 16 W 275 nm lamp set by circular arrangement eight of 2 W LED lights in series, irradiation for 2 min, Ar atmosphere, room temperature, stir 800 rpm.

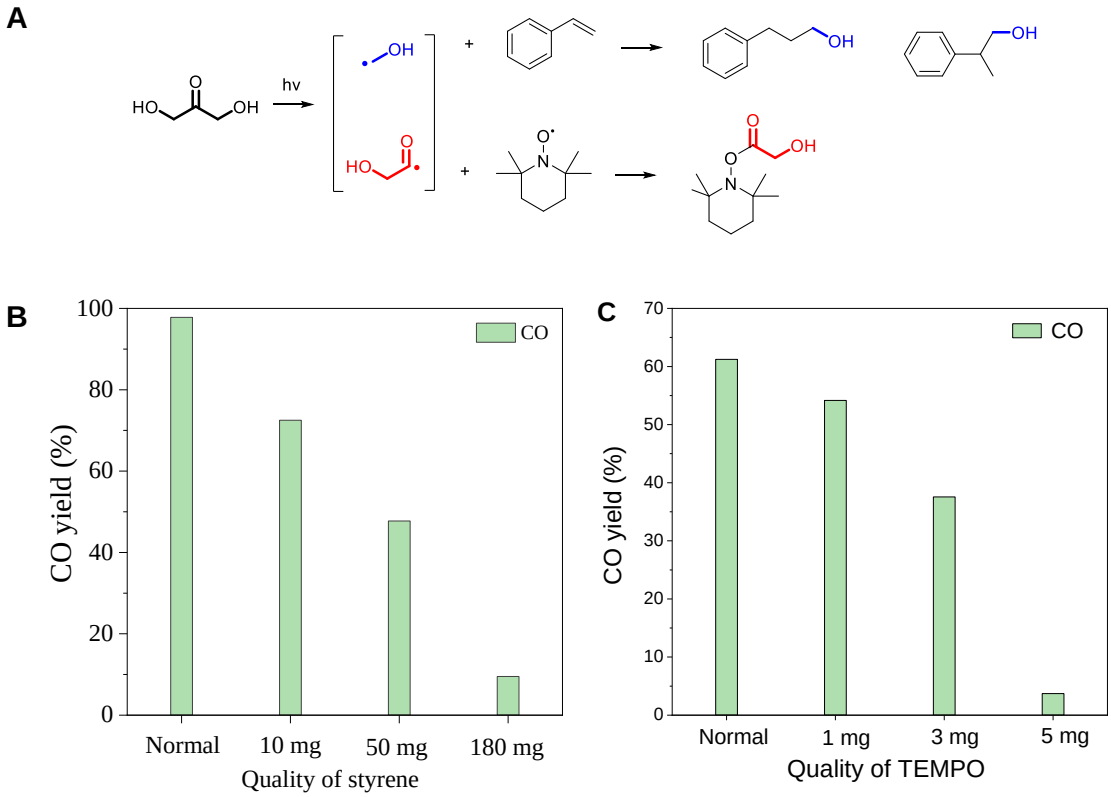

Fig. S9. Radical trapping experiments. (A) Capture reaction mechanisms. (B) The CO yield for the photolysis of DHA with adding different quantities of styrene. (C) The CO yield for the photolysis of DHA with adding different quantities of TEMPO. Reaction conditions with adding styrene: 0.1 M DHA, 1 mL of MeCN and H_2O (the volume ratio is 9 : 1), home-made 16 W 275 nm lamp set by circular arrangement eight of 2 W LED lights in series, irradiation for 2 h, Ar atmosphere, room temperature, stir 800 rpm. Reaction conditions with adding TEMPO: 0.1 M DHA, 1 mL of MeCN and H_2O (the volume ratio is 9 : 1), home-made 16 W 275 nm lamp set by circular arrangement eight of 2 W LED lights in series, irradiation for 5 min, Ar atmosphere, room temperature, stir 800 rpm.

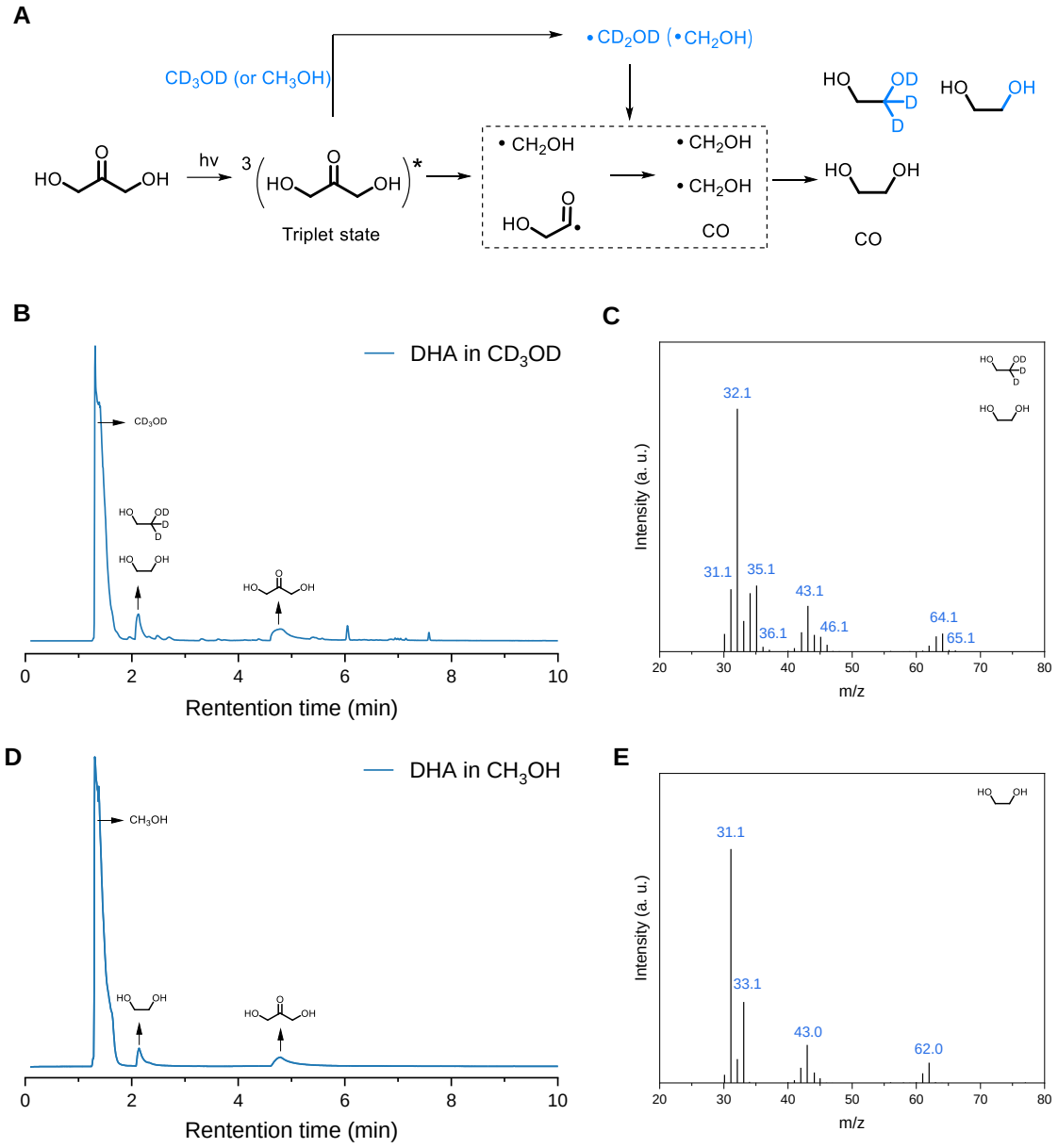

Fig. S10. Photolysis of DHA in deuterated methanol or methanol. (A) Activation of hydrocarbon bonds and intermolecular crossover reaction. (B, D) GC-MS patterns for the photolysis of DHA in deuterated methanol or methanol. (C, E) MS spectra in GC-MS pattern at a retention time of about 2.2 min for EG or deuterated EG. Reaction conditions: 0.1 M DHA, 1 mL of CD_3OD or CH_3OH, home-made 16 W 275 nm lamp set by circular arrangement eight of 2 W LED lights in series, irradiation for 1 h, Ar atmosphere, room temperature, stir 800 rpm.

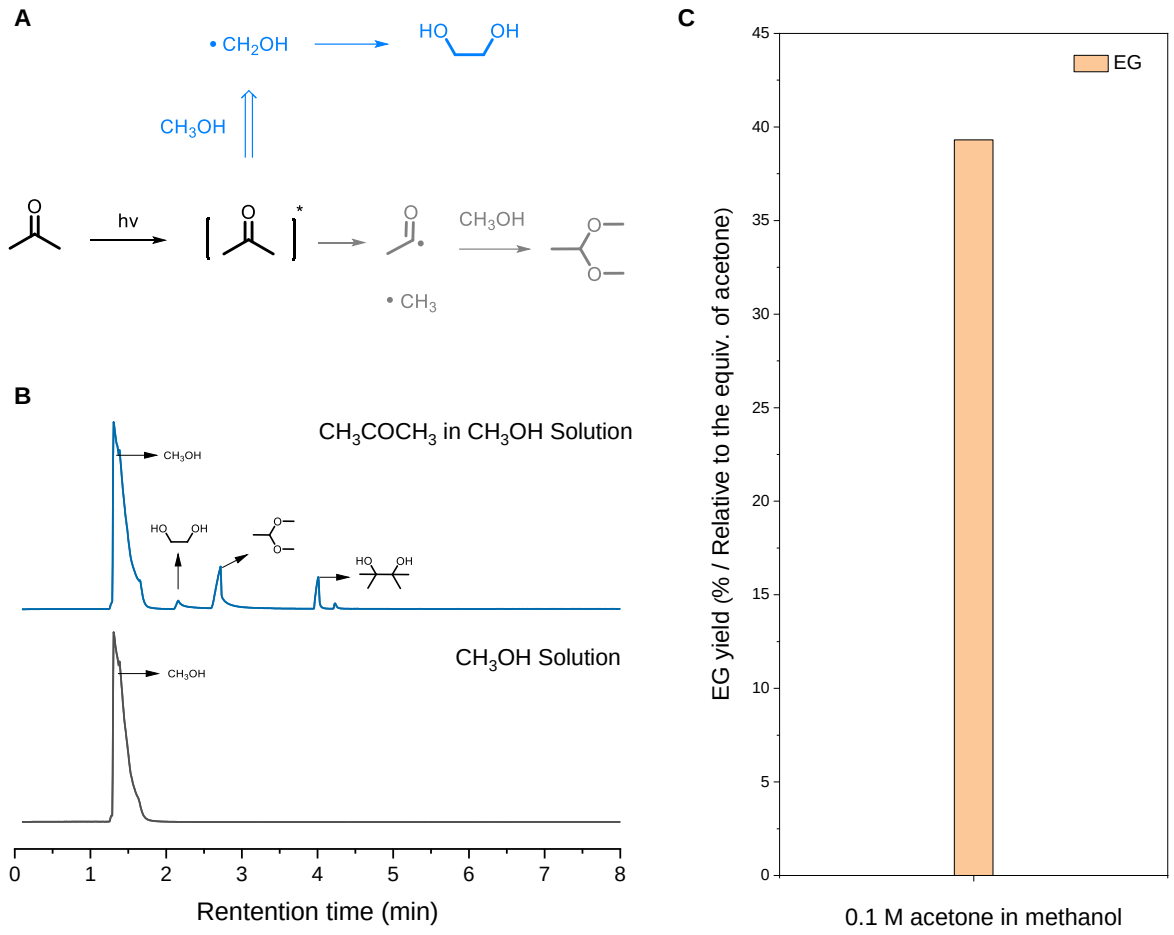

Fig. S11. Photolysis of acetone in methanol. (A) Activation of hydrocarbon bonds of methanol and C-C bond coupling of hydroxymethyl radical. (B) GC-MS patterns for the photolysis of acetone in methanol or only methanol. (C) The EG yield relative to the amount of acetone added. Normal conditions: 0.1 M acetone, 1 mL of CH_3OH, home-made 16 W 275 nm lamp set by circular arrangement eight of 2 W LED lights in series, irradiation for 1 h, Ar atmosphere, room temperature, stir 800 rpm.

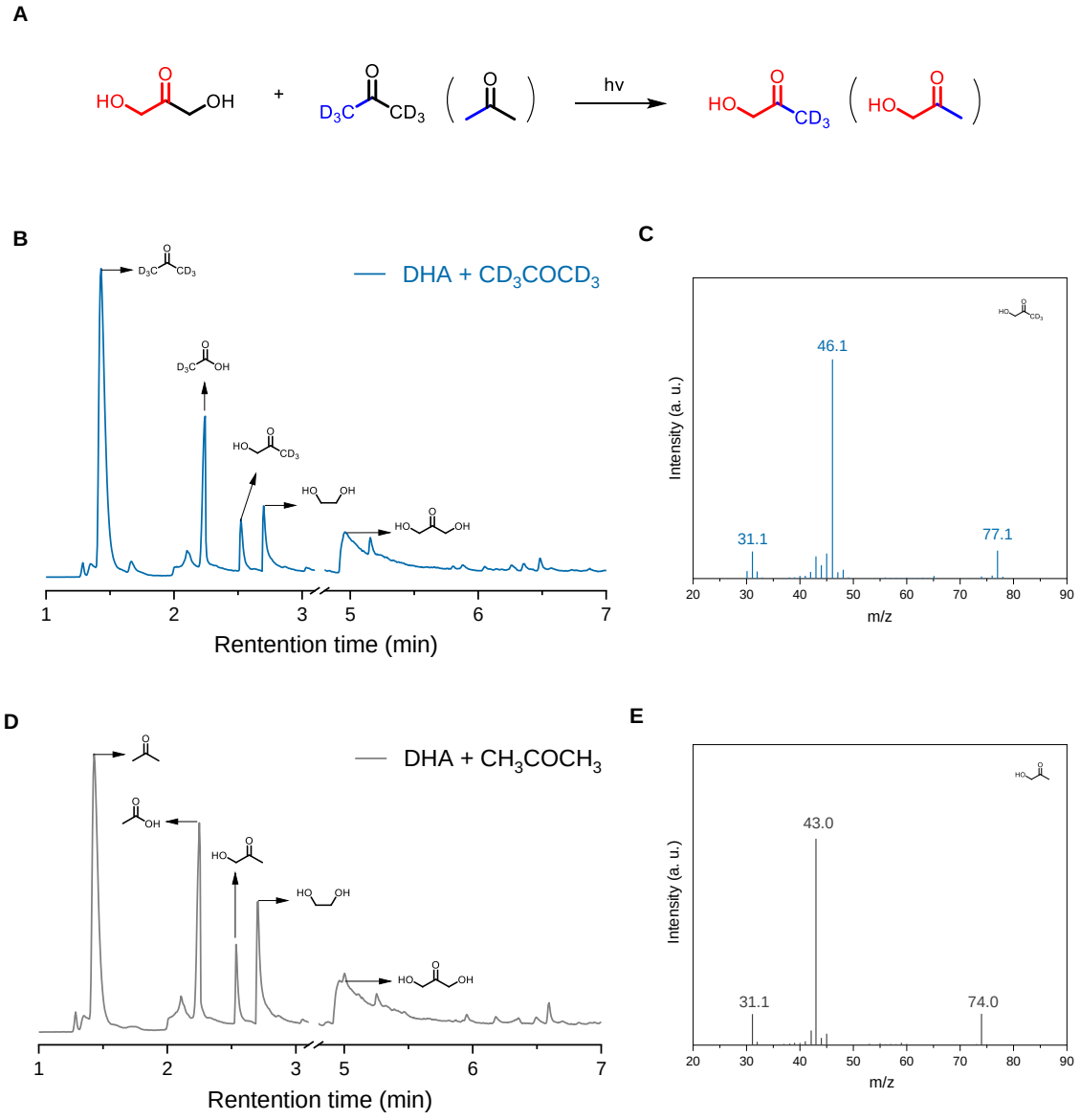

Fig. S12. Photolysis of DHA and (deuterated) acetone in water solution. (A) Intermolecular crossover reaction. (B, D) GC-MS patterns for the photolysis of DHA and (deuterated) acetone in water solution. (C, E) MS spectra in GC-MS pattern at a retention time of about 2.55 min for hydroxyacetone or deuterated hydroxyacetone. Reaction conditions: 0.1 M DHA and 0.1 M (deuterated) acetone, 1 mL of H2O, home-made 16 W 275 nm lamp set by circular arrangement eight of 2 W LED lights in series, irradiation for 1 h, Ar atmosphere, room temperature, stir 800 rpm.

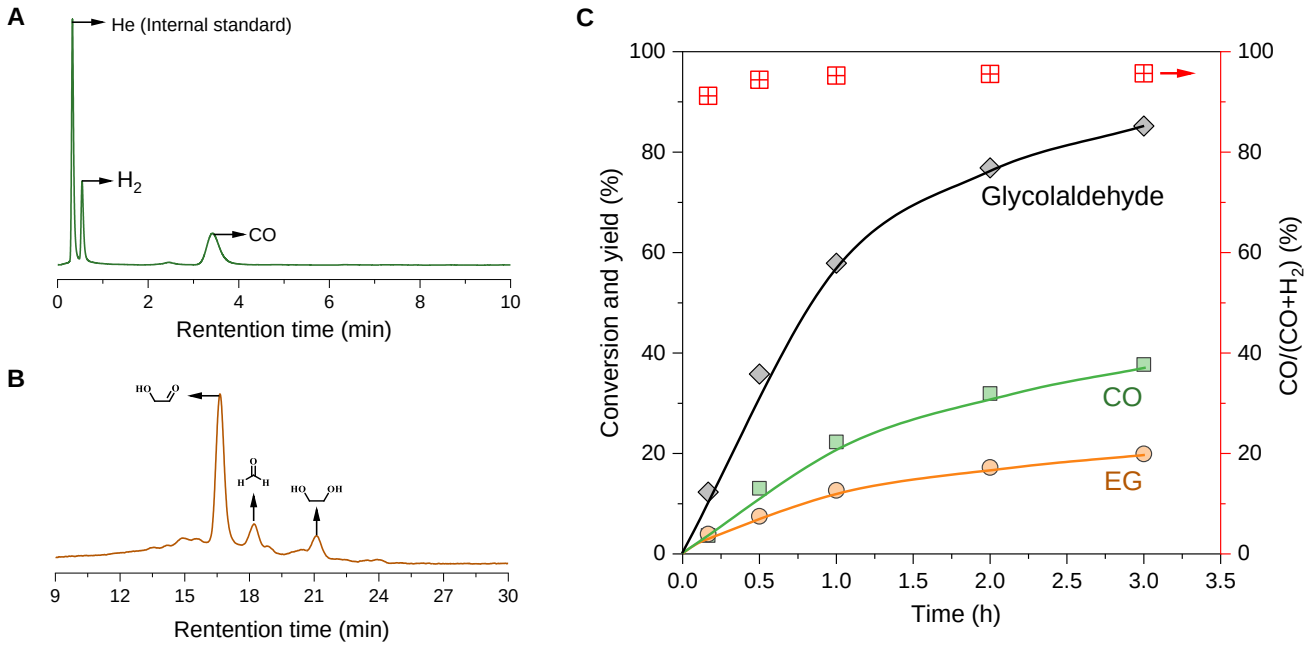

Fig. S13. Photolysis of glycolaldehyde. (A) Gas chromatogram after 1 h. (B) The high-performance liquid chromatogram after 1 h. (C) Time-dependent profile. Reaction conditions: 0.1 M glycolaldehyde, 1 mL of H_2O, home-made 16 W 275 nm lamp set by circular arrangement eight of 2 W LED lights in series, irradiation for 0-3 h, Ar atmosphere, room temperature, stir 800 rpm.

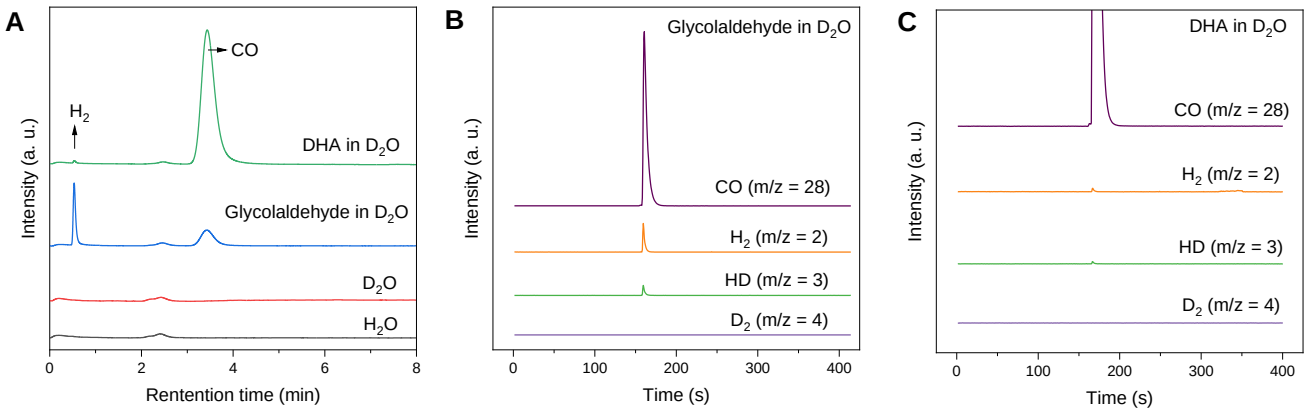

Fig. S14. Photolysis of DHA and glycolaldehyde in D_2O or photolysis of D_2O and water. (A) Gas chromatograms for photolysis of DHA and glycolaldehyde in D_2O or photolysis of only D_2O and water. (B) Online mass spectrometer chromatograms of photolysis of glycolaldehyde in D_2O obtained by ex situ injection detection. (C) Online mass spectrometer chromatograms of photolysis of DHA in D_2O obtained by ex situ injection detection. Reaction conditions: 0.1 M DHA or glycolaldehyde or no substrates, 1 mL of H_2O, home-made 16 W 275 nm lamp set by circular arrangement eight of 2 W LED lights in series, irradiation for 1 h, Ar atmosphere, room temperature, stir 800 rpm.

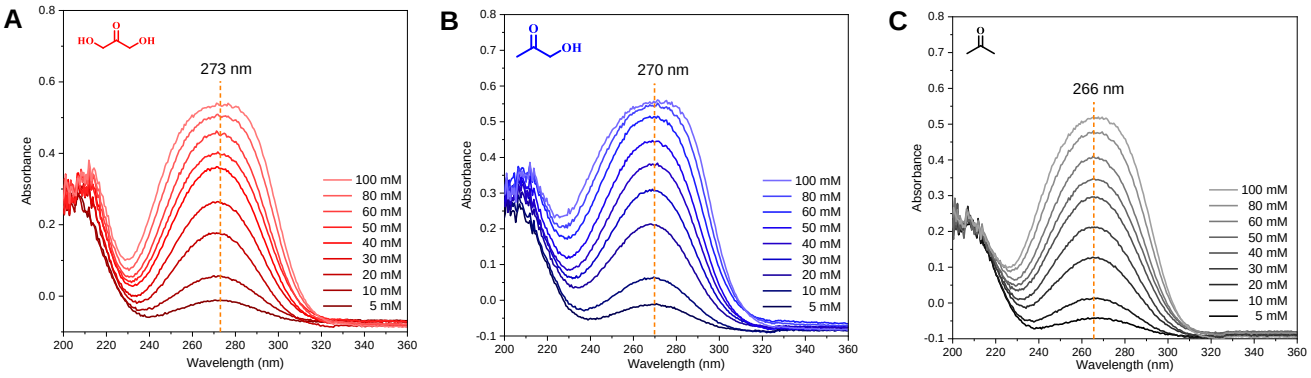

Fig. S15. UV-Vis diffuse reflectance spectra of (A) dihydroxyacetone, (B) hydroxyacetone, and (C) acetone.

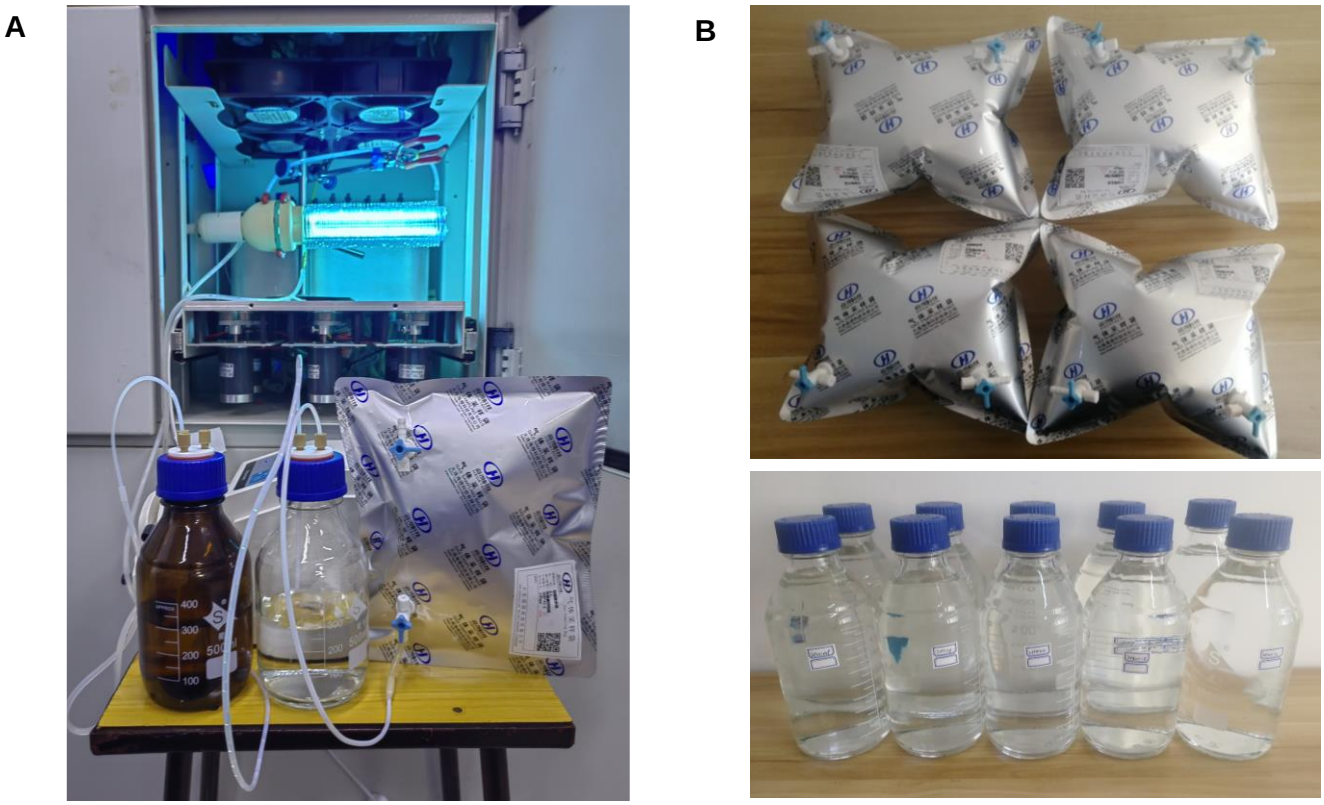

Fig. S16. Home-built photochemical flow device. (A) The working photochemical flow reaction device. (B) Partial collected CO and EG aqueous solution during DHA photolysis for 1000 h.

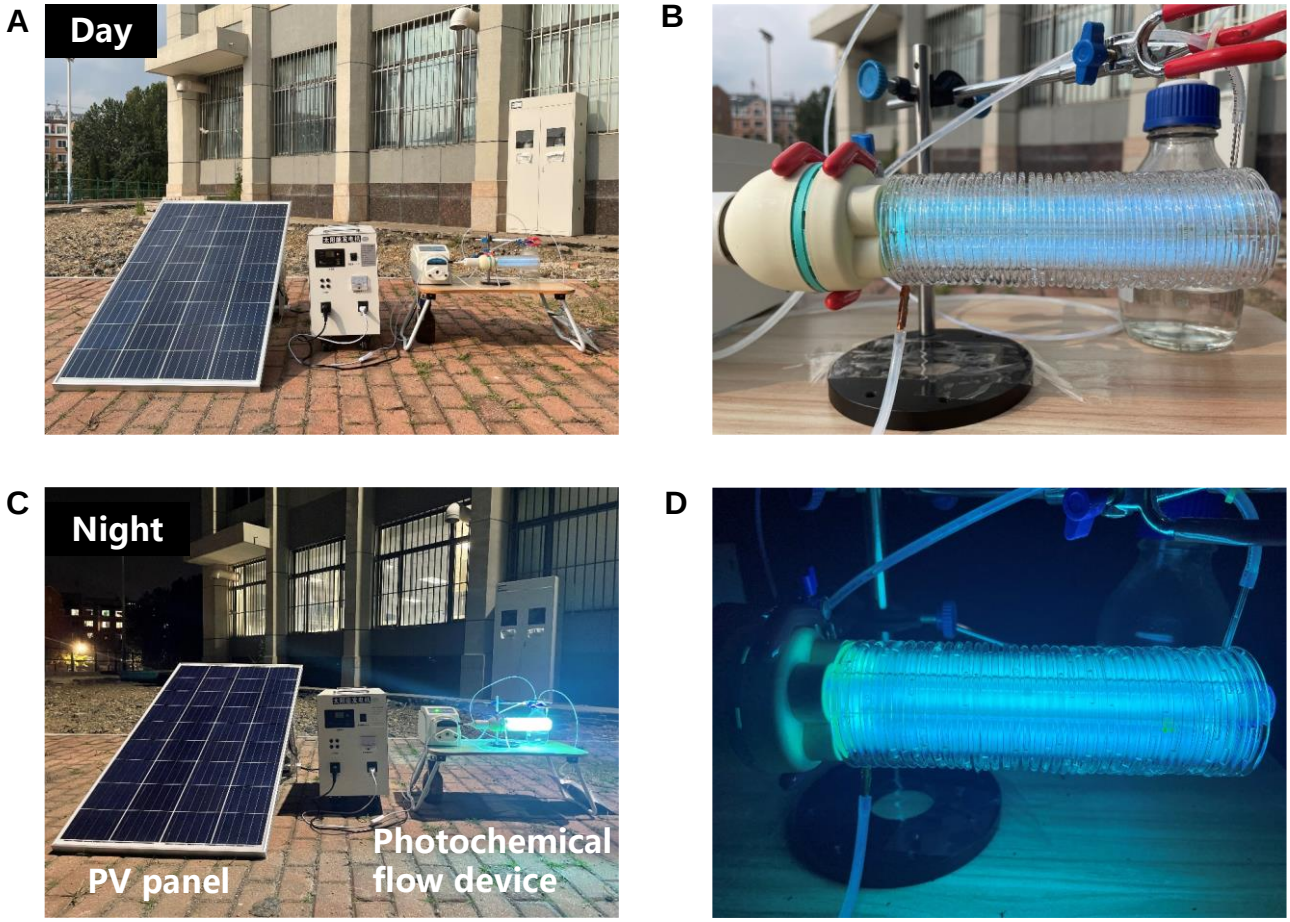

Fig. S17. Home-built Sunlight-Electricity-Ultraviolet light system. (A, C) Sunlight-Electricity-Ultraviolet light system composed of photovoltaic panel, power storage and photochemical flow device working day and night. (B, D) Spiral quartz tube that surrounding the ultraviolet lamp working day and night.

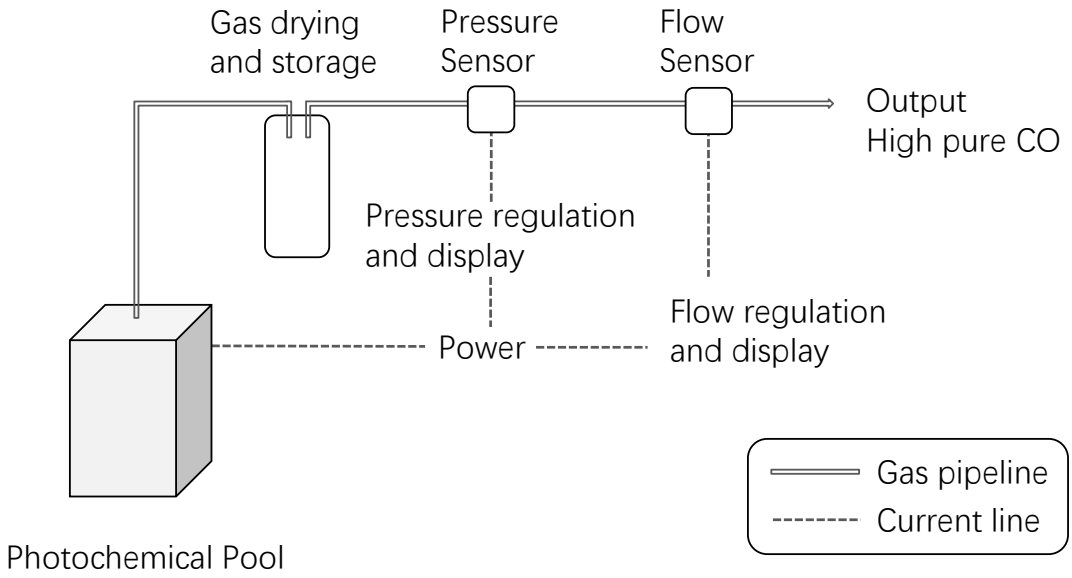

Fig. S18. Brief working principle diagram for CO Generator.

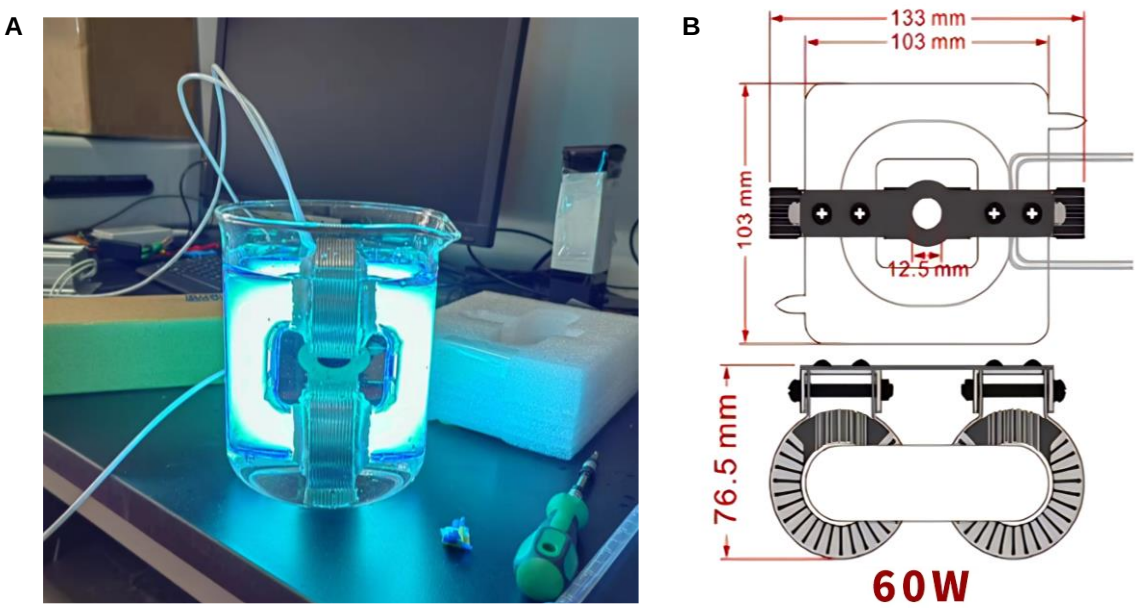

Fig. S19. Non-polar submersible UV lamp. (A) the photo and (B) size specification.

References

1 Frisch, M. J. *et al.* Gaussian 09, Revision B.01. (2010).

2 Roothaan, C. C. J. New Developments in Molecular Orbital Theory. *Rev. Mod. Phys.* **23**, 69-89, (1951).

3 Head-Gordon, M., Pople, J. A. & Frisch, M. J. MP2 energy evaluation by direct methods. *Chem. Phys. Lett.* **153**, 503-506, (1988).

4 Hohenberg, P. & Kohn, W. Inhomogeneous Electron Gas. *Phys. Rev.* **136**, B864-B871, (1964).

5 Grimme, S. Accurate description of van der Waals complexes by density functional theory including empirical corrections. *J. Comput. Chem.* **25**, 1463-1473, (2004).

6 Becke, A. D. Density-functional exchange-energy approximation with correct asymptotic behavior. *Phys. Rev. A* **38**, 3098-3100, (1988).

7 Xia, Y.-S. *et al.* Tandem utilization of CO_2 photoreduction products for the carbonylation of aryl iodides. *Nat. Commun.* **13**, 2964, (2022).

8 Iizuka, M. & Kondo, Y. Remarkable ligand effect on the palladium-catalyzed double carbonylation of aryl iodides. *Chem. Commun.* 1739, (2006).

9 Losch, P., Felten, A.-S. & Pale, P. Easy, Green and Safe Carbonylation Reactions through Zeolite-Catalyzed Carbon Monoxide Production from Formic Acid. *Adv. Synth. Catal.* **357**, 2931-2938, (2015).

10 Neumann, K. T., Laursen, S. R., Lindhardt, A. T., Bang-Andersen, B. & Skrydstrup, T. Palladium-Catalyzed Carbonylative Sonogashira Coupling of Aryl Bromides Using Near Stoichiometric Carbon Monoxide. *Org. Lett.* **16**, 2216-2219, (2014).

11 Ahlburg, A., Lindhardt, A. T., Taaning, R. H., Modvig, A. E. & Skrydstrup, T. An Air-Tolerant Approach to the Carbonylative Suzuki–Miyaura Coupling: Applications in Isotope Labeling. *J. Org. Chem.* **78**, 10310-10318, (2013).

12 Liang, B. *et al.* Pd-Catalyzed Copper-Free Carbonylative Sonogashira Reaction of Aryl Iodides with Alkynes for the Synthesis of Alkynyl Ketones and Flavones by Using Water as a Solvent. *J. Org. Chem.* **70**, 6097-6100, (2005).

13 Thomas, J. S. G. The Complete Gasification of Coal. *Nature* **111**, 778-779, (1923).

14 Shafirovich, E. & Varma, A. Underground Coal Gasification: A Brief Review of Current Status. *Ind. Eng. Chem. Res.* **48**, 7865-7875, (2009).

15 Wall, D., Kepplinger, W. & Millner, R. Smelting-Reduction Export Gas as Syngas in the Chemical Industry. *Steel Res. Int.* **82**, 926-933, (2011).

16 Wang, F. *et al.* A novelty catalytic reforming of tire pyrolysis oil for hydrogen-rich syngas. *Energy Convers.* **300**, 117925, (2024).

17 Huber, G. W., Iborra, S. & Corma, A. Synthesis of Transportation Fuels from Biomass: Chemistry, Catalysts, and Engineering. *Chem. Rev.* **106**, 4044-4098, (2006).

18 Patra, T. K. & Sheth, P. N. Biomass gasification coupled with producer gas cleaning, bottling and HTS catalyst treatment for H_2-rich gas production. *Int. J. Hydrogen Energy* **44**, 11602-11616, (2019).

19 Luque, R. *et al.* Design and development of catalysts for Biomass-To-Liquid-Fischer–Tropsch (BTL-FT) processes for biofuels production. *Energy Environ. Sci.* **5**, 5186-5202, (2012).

20 Buelens, L. C., Galvita, V. V., Poelman, H., Detavernier, C. & Marin, G. B. Super-dry reforming of methane intensifies CO_2 utilization via Le Chatelier's principle. *Science* **354**, 449-452, (2016).

21 Haug, L. *et al.* Zirconium Carbide Mediates Coke-Resistant Methane Dry Reforming on Nickel-Zirconium Catalysts. *Angew. Chem. Int. Ed.* **61**, e202213249 (2022).

22 Hickman, D. A. & Schmidt, L. D. Production of Syngas by Direct Catalytic Oxidation of Methane. *Science* **259**, 343-346, (1993).

23 Palmer, C. *et al.* Dry reforming of methane catalysed by molten metal alloys. *Nat. Catal.* **3**, 83-89, (2020).

24 Parsapur, R. K., Chatterjee, S. & Huang, K.-W. The Insignificant Role of Dry Reforming of Methane in CO_2 Emission Relief. *ACS Energy Lett.* **5**, 2881-2885, (2020).

25 Jung, S., Lee, J., Moon, D. H., Kim, K.-H. & Kwon, E. E. Upgrading biogas into syngas through dry reforming. *Renew. Sust. Energ. Rev.* **143**, 110949, (2021).

26 Porosoff, M. D., Yan, B. & Chen, J. G. Catalytic reduction of CO_2 by H_2 for synthesis of CO, methanol and hydrocarbons: challenges and opportunities. *Energy Environ. Sci.* **9**, 62-73, (2016).

27 Li, S. *et al.* Tuning the CO_2 Hydrogenation Selectivity of Rhodium Single-Atom Catalysts on Zirconium Dioxide with Alkali Ions. *Angew. Chem. Int. Ed.* **62**, e202218167 (2023).

28 Yang, Q. *et al.* Activity and selectivity descriptors for iron carbides in CO_2 hydrogenation. *Appl. Catal. B: Environ.* **327**, 122450, (2023).

29 Wei, X. *et al.* Surfactants Used in Colloidal Synthesis Modulate Ni Nanoparticle Surface Evolution for Selective CO_2 Hydrogenation. *J. Am. Chem. Soc.* **145**, 14298-14306, (2023).

30 Kim, J. Y. T. *et al.* Recovering carbon losses in CO_2 electrolysis using a solid electrolyte reactor. *Nat. Catal.* **5**, 288-299, (2022).

31 Jung, H. *et al.* Continuous-flow reactor with superior production rate and stability for CO_2 reduction using semiconductor photocatalysts. *Energy Environ. Sci.* **16**, 2869-2878, (2023).

32 Dye, R. F. Ethylene glycols technology. *Korean J. Chem. Eng.* **18**, 571-579, (2001).

33 Pu, T., Tian, H., Ford, M. E., Rangarajan, S. & Wachs, I. E. Overview of Selective Oxidation of Ethylene to Ethylene Oxide by Ag Catalysts. *ACS Catal.* **9**, 10727-10750, (2019).

34 Ye, R.-P. *et al.* Perspectives on the Active Sites and Catalyst Design for the Hydrogenation of Dimethyl Oxalate. *ACS Catal.* **10**, 4465-4490, (2020).

35 Zheng, J. *et al.* Ambient-pressure synthesis of ethylene glycol catalyzed by C60-buffered Cu/SiO_2. *Science* **376**, 288-292, (2022).

36 Wang, A. & Zhang, T. One-Pot Conversion of Cellulose to Ethylene Glycol with Multifunctional Tungsten-Based Catalysts. *Acc. Chem. Res.* **46**, 1377-1386, (2013).

37 Liu, W. *et al.* A Durable Nickel Single-Atom Catalyst for Hydrogenation Reactions and Cellulose Valorization under Harsh Conditions. *Angew. Chem. Int. Ed.* **57**, 7071-7075, (2018).

38 Ji, N. *et al.* Direct Catalytic Conversion of Cellulose into Ethylene Glycol Using Nickel-Promoted Tungsten Carbide Catalysts. *Angew. Chem. Int. Ed.* **47**, 8510-8513, (2008).

39 Xie, S. *et al.* Visible light-driven C-H activation and C-C coupling of methanol into ethylene glycol. *Nat. Commun.* **9**, 1181, (2018).

40 Wang, L. *et al.* Precisely Constructed Metal Sulfides with Localized Single-Atom Rhodium for Photocatalytic C−H Activation and Direct Methanol Coupling to Ethylene Glycol. *Adv. Mater.* **35**, 2205782, (2022).